LHC/γC Complementarity in Probing the Scalar Sector of the Randall-Sundrum Model

Jack Gunion
Davis Institute for High Energy Physics, U.C. Davis

Collaborators: M. Battaglia, S. de Curtix, A. De Roeck, D. Dominici, B. Grzadkowski, M. Toharia, J. Wells

γC Video Conf., 6/26/2003

Outline

- The parameter space
- Basics of the couplings
- LHC/γC Complementarity
- Conclusions

Presuming the new physics scale to be close to the TeV scale, there can be a rich new phenomenology in which Higgs and radion physics intermingle if the $\xi R\widehat{H}^\dagger\widehat{H}$ mixing term is present in $\mathcal{L}$.
References:

- D. Dominici, B. Grzadkowski, J. F. Gunion and M. Toharia, "The scalar sector of the Randall-Sundrum model," arXiv:hep-ph/0206192.
- M. Battaglia, S. De Curtis, A. De Roeck, D. Dominici and J. F. Gunion, "On the complementarity of Higgs and radion searches at LHC," arXiv:hep-ph/0304245.

- **D. M. Asner, J. B. Gronberg and J. F. Gunion, "Detecting and studying Higgs bosons in two-photon collisions at a linear collider," Phys. Rev. D 67, 035009 (2003) [arXiv:hep-ph/0110320].**

Randal-Sundrum Review

Some possibly very dramatic changes in phenomenology.

- There are two branes, separated in the 5th dimension (y) and $y \to -y$ symmetry is imposed. With appropriate boundary conditions, the 5D Einstein equations $\Rightarrow$

$$ds^2 = e^{-2\sigma(y)}\eta_{\mu\nu}dx^\mu dx^\nu - b_0^2 dy^2, \tag{1}$$

  where $\sigma(y) \sim m_0 b_0 |y|$.

- $e^{-2\sigma(y)}$ is the warp factor; scales at $y = 0$ of order M_{Pl} on the hidden brane are reduced to scales at $y = 1/2$ of order TeV on the visible brane.

- Fluctuations of $g_{\mu\nu}$ relative to $\eta_{\mu\nu}$ are the KK excitations $h^n_{\mu\nu}$.

- Fluctuations of $b(x)$ relative to b_0 define the radion field.

- In addition, we place a Higgs doublet $\widehat{H}$ on the visible brane. After various rescalings, the properly normalized quantum fluctuation field is called h_0.

Including the ξ mixing term

- We begin with

$$S_\xi = \xi \int d^4x \sqrt{g_{\rm vis}} R(g_{\rm vis}) \widehat{H}^\dagger \widehat{H} \,, \tag{2}$$

where $R(g_{\rm vis})$ is the Ricci scalar for the metric induced on the visible brane.

- A crucial parameter is the ratio

$$\gamma \equiv v_0/\Lambda_\phi \,. \tag{3}$$

where Λ_ϕ is vacuum expectation value of the radion field.

- After writing out the full quadratic structure of the Lagrangian, including $\xi \neq 0$ mixing, we obtain a form in which the h_0 and ϕ_0 fields for $\xi = 0$ are mixed and have complicated kinetic energy normalization.

  We must diagonalize the kinetic energy and rescale to get canonical

normalization.

$$h_0 = \left(\cos\theta - \frac{6\xi\gamma}{Z}\sin\theta\right) h + \left(\sin\theta + \frac{6\xi\gamma}{Z}\cos\theta\right)\phi$$
$$\equiv dh + c\phi \tag{4}$$
$$\phi_0 = -\cos\theta\frac{\phi}{Z} + \sin\theta\frac{h}{Z} \equiv a\phi + bh\,. \tag{5}$$

- In the above equations

$$Z^2 \equiv 1 + 6\xi\gamma^2(1 - 6\xi)\,. \tag{6}$$

$Z^2 > 0$ is required to avoid tachyonic situation.

This $\Rightarrow$ constraint on maximum neg. and pos. ξ values.

- The process of inversion is very critical to the phenomenology and somewhat delicate.

The result found is that the physical mass eigenstates h and ϕ cannot be too close to being degenerate in mass, depending on the precise values of ξ and γ; extreme degeneracy is allowed only for small ξ and/or γ.

Using this inversion, for given ξ, γ, m_h and m_ϕ we compute Z^2, $m^2_{h_0}$ and $m^2_{\phi_0}$, θ to obtain a, b, c, d in Eqs. (4) and (5).

- **Net result**

  4 independent parameters to completely fix the mass diagonalization of the scalar sector when $\xi \neq 0$. These are:

$$\xi\,, \quad \gamma\,, \quad m_h\,, \quad m_\phi\,, \tag{7}$$

  where we recall that $\gamma \equiv v_0/\Lambda_\phi$ with $v_0 = 246$ GeV.

  Two additional parameters will be required to completely fix the phenomenology of the scalar sector, including all possible decays. These are

$$\widehat{\Lambda}_W\,, \quad m_1\,, \tag{8}$$

  where $\widehat{\Lambda}_W$ will determine KK-graviton couplings to the h and ϕ and m_1 is the mass of the first KK graviton excitation.

There are relations among parameters:

$$\widehat{\Lambda}_W \simeq \sqrt{2} M_{Pl} \Omega_0 \,, \quad m_n = m_0 x_n \Omega_0 \,, \quad \Lambda_\phi = \sqrt{6} M_{Pl} \Omega_0 = \sqrt{3} \widehat{\Lambda}_W \tag{9}$$

where $\Omega_0 M_{Pl} = e^{-m_0 b_0/2} M_{Pl}$ should be of order a TeV to solve the hierarchy problem. In Eq. (9), the x_n are the zeroes of the Bessel function J_1 ($x_1 \sim 3.8$, $x_2 \sim 7.0$). A useful relation following from the above equations is:

$$m_1 = x_1 \frac{m_0}{M_{Pl}} \frac{\Lambda_\phi}{\sqrt{6}} \,. \tag{10}$$

m_0/M_{Pl} is related to the curvature of the brane and should be a relatively small number for consistency of the RS scenario.

- Sample parameters that are safe from precision EW data and RunI Tevatron constraints are $\Lambda_\phi = 5$ TeV ($\Rightarrow \widehat{\Lambda}_W \sim 3$ TeV) and $m_0/M_{Pl} = 0.1$.

  The latter $\Rightarrow m_1 \sim 780$ GeV; i.e. m_1 is typically too large for KK graviton excitations to be present, or if present, important, in h, ϕ decays.

  But, KK excitations themselves will be observed and well measured at the LHC.

- Given this choice, we complete the inversion by writing out the kinetic energy terms of the complete Lagrangian using the substitutions of Eqs. (4) and (5) and demanding that the coefficients of $-\frac{1}{2}h^2$ and $-\frac{1}{2}\phi^2$ agree with the given input values for m_h^2 and m_ϕ^2.

  Results shown take $m_0/M_{Pl} = 0.1$.

- KK excitation probably observable at LHC

  Will provide important information.

  1. Mass gives m_1 in above notation.
  2. Excitation spectrum as a function of m_{jj} determines m_0/M_{Pl}.
  3. Combine ala Eq. (10) to get Λ_ϕ.
     This will really help in LHC-only study of Higgs sector.

The Couplings

The $f\overline{f}$ and VV couplings

- **The VV couplings**
  - The h_0 has standard ZZ coupling.
  - The ϕ_0 has ZZ coupling deriving from the interaction $-\frac{\phi_0}{\Lambda_\phi}T^\mu_\mu$ using the covariant derivative portions of $T^\mu_\mu(h_0)$.

  The result for the $\eta_{\mu\nu}$ portion of the ZZ couplings is:

$$g_{ZZh} = \frac{g\, m_Z}{c_W}(d + \gamma b)\ , \quad g_{ZZ\phi} = \frac{g\, m_Z}{c_W}(c + \gamma a)\ . \tag{11}$$

  g and c_W denote the $SU(2)$ gauge coupling and $\cos\theta_W$, respectively. The WW couplings are obtained by replacing gm_Z/c_W by gm_W.

- **The $f\overline{f}$ couplings**
  - The h_0 has standard fermionic couplings.

- The fermionic couplings of the ϕ_0 derive from $-\frac{\phi_0}{\Lambda_\phi} T^\mu_\mu$ using the Yukawa interaction contributions to T^μ_μ.
- One obtains results in close analogy to the VV couplings just considered:

$$g_{f\bar{f}h} = -\frac{g\, m_f}{2\, m_W}(d + \gamma b)\,, \quad g_{f\bar{f}\phi} = -\frac{g\, m_f}{2\, m_W}(c + \gamma a)\,. \tag{12}$$

- Note same factors for WW and $f\bar{f}$ couplings.

The gg and $\gamma\gamma$ couplings

- There are the standard loop contributions, except rescaled by $f\bar{f}/VV$ strength factors g_{fVh} or $g_{fV\phi}$.

- In addition, there are anomalous contributions, which are expressed in terms of the SU(3)×SU(2)×U(1) β function coefficients $b_3 = 7$, $b_2 = 19/6$ and $b_Y = -41/6$.

- The anomalous couplings of h and ϕ enter only through their radion admixtures, $g_h = \gamma b$ for the h, and $g_\phi = \gamma a$ for the ϕ.

Couplings

- First, consider the $f\overline{f}/VV$ couplings of h and ϕ relative to SM, taking $m_h = 120$ GeV and $\Lambda_\phi = 5$ TeV.

- **The most important points**

  If $g^2_{fVh} < 1$ is observed then $m_\phi > m_h$, and vice versa, except for small region near $\xi = 0$.

  In cases where $g_{fV\phi}$ is small, prior indirect knowledge of, or constraints on, m_ϕ could be crucial.

  At large $|\xi|$, if $m_\phi > m_h$ the $ZZ\phi$ couplings can become sort of SM strength, implying SM type discovery modes could become relevant.

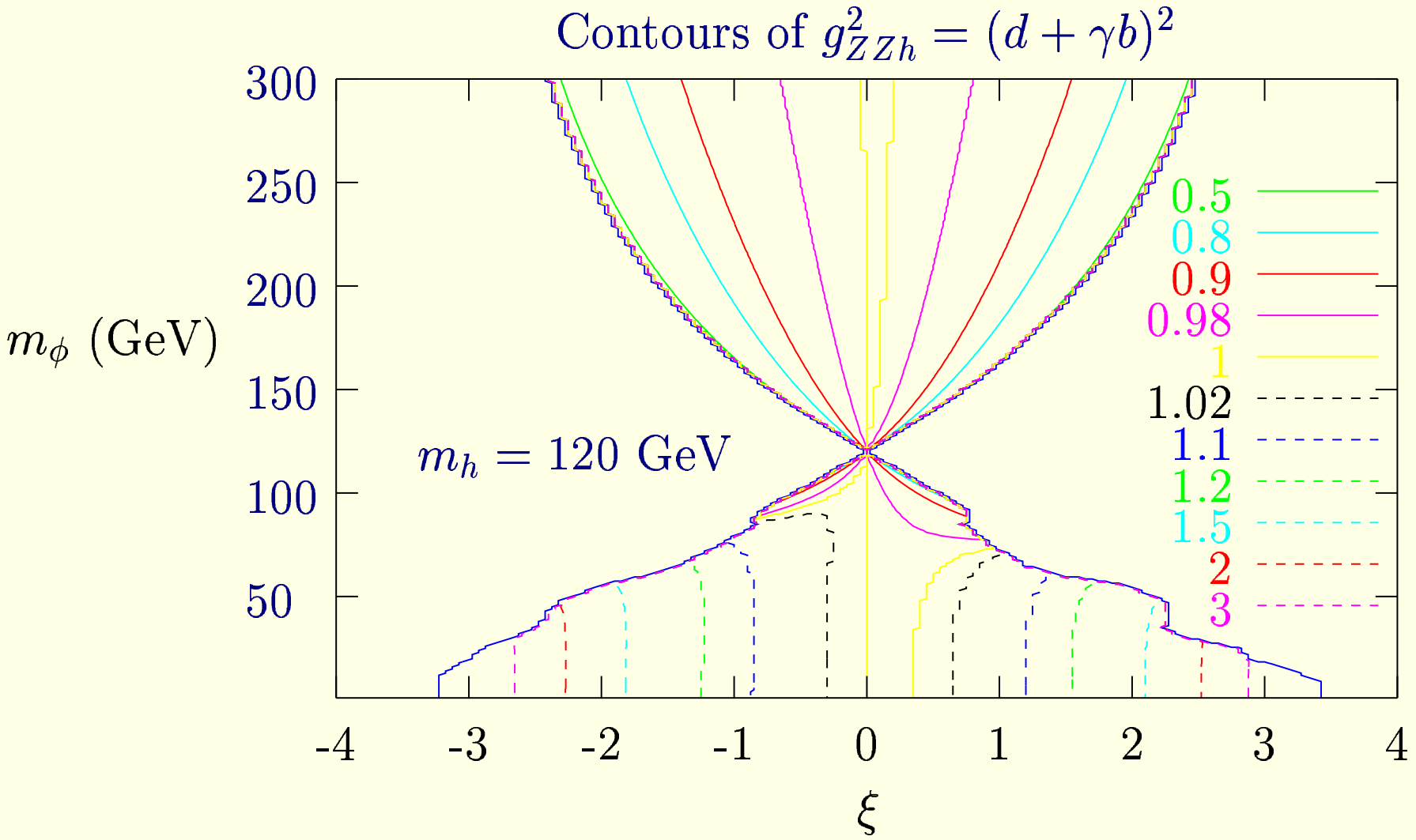

Figure 1: *Contours of* g^2_{fVh} *(relative to SM) for* $\Lambda_\phi = 5$ TeV, $m_h = 120$ GeV.

- **Observe suppression if** $m_\phi > m_h$ **and vice versa.**

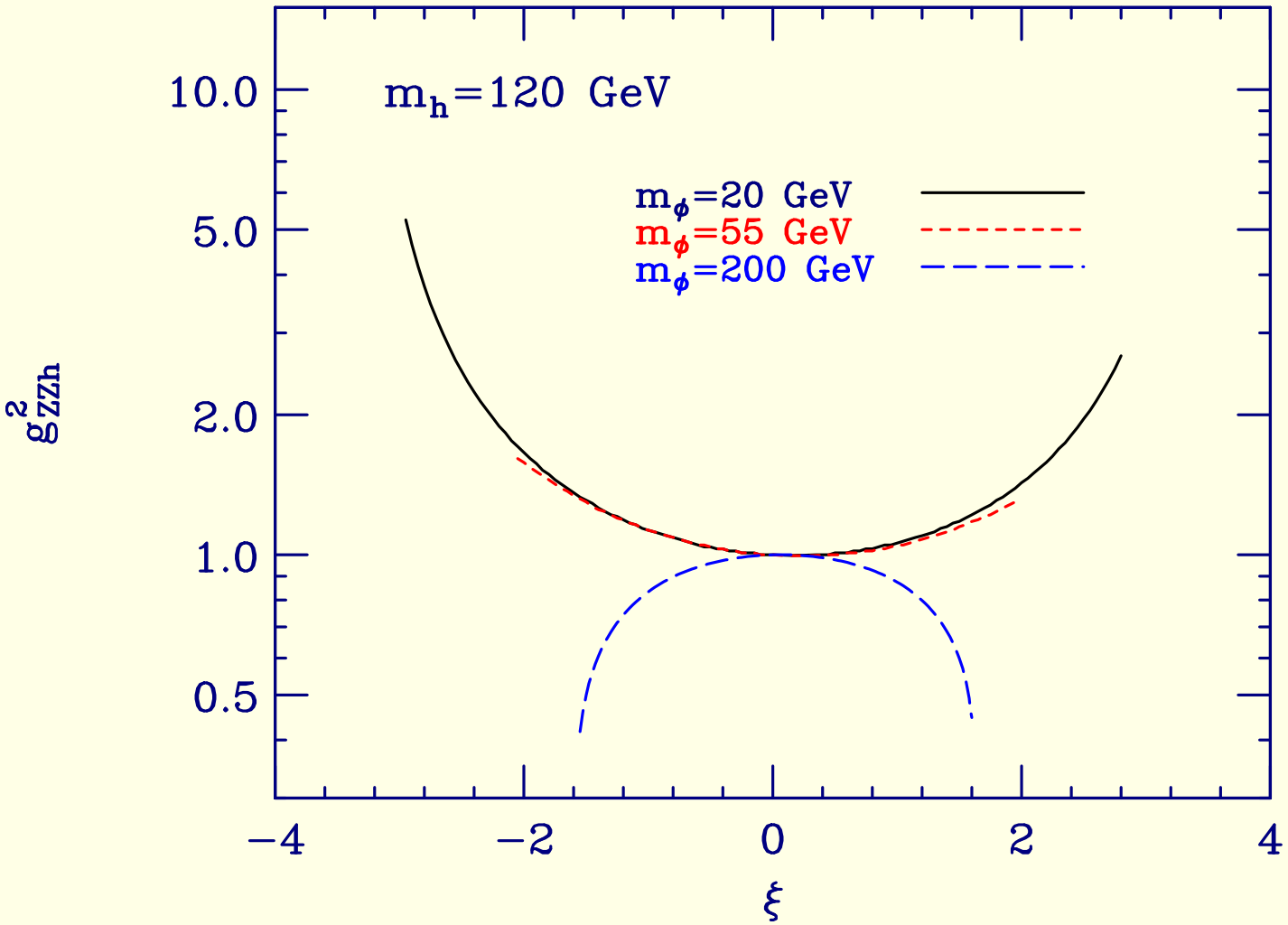

Figure 2: $g^2_{ZZh}/g^2_{ZZh_{\rm SM}} = g^2_{f\bar{f}h}/g^2_{f\bar{f}h_{\rm SM}}$ *as a function of* ξ *for several* m_ϕ *values.*

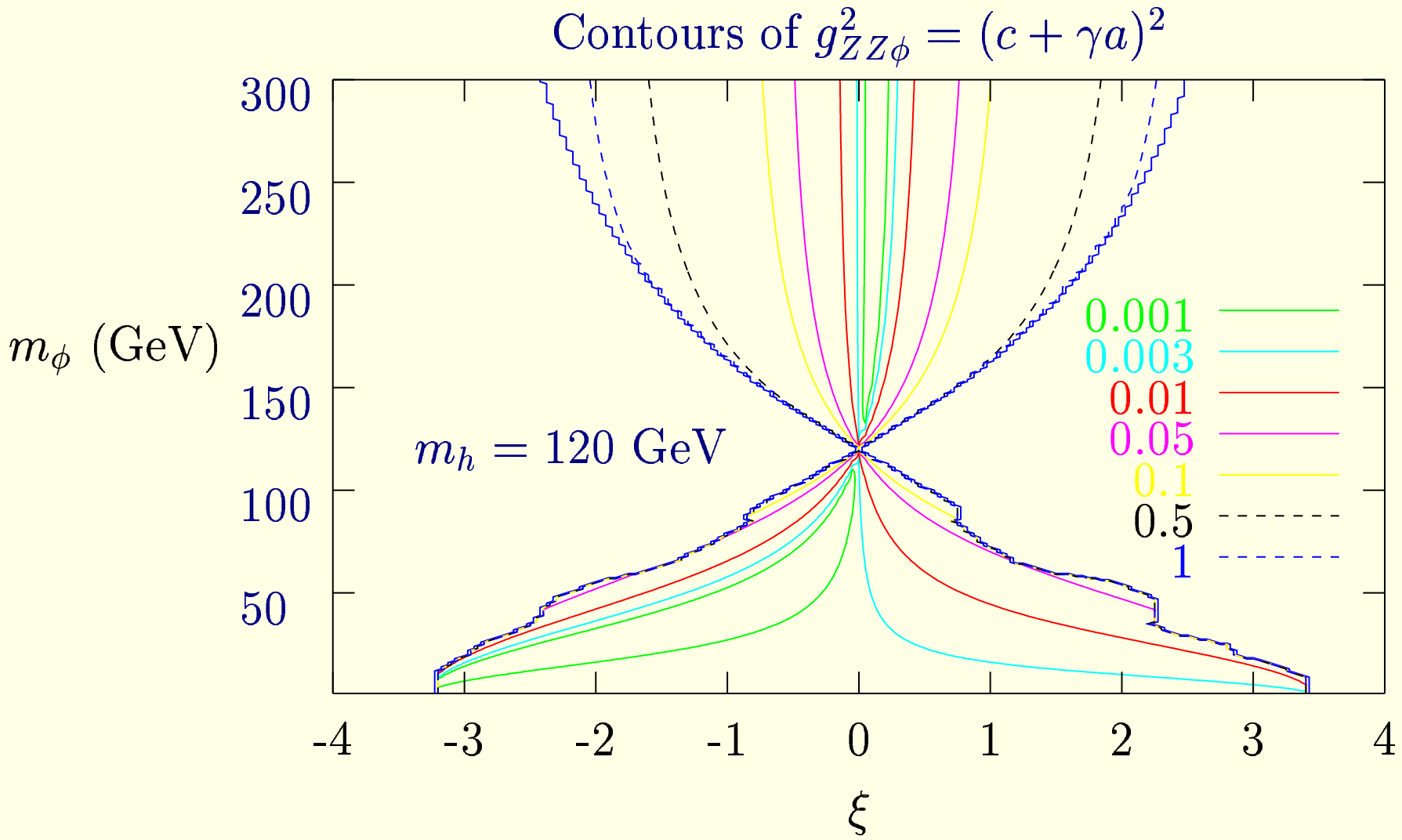

Figure 3: *Contours of* $g^2_{fV\phi}$ *for* $\Lambda_\phi = 5$ TeV, $m_h = 120$ GeV

- **Substantial** $g^2_{fV\phi}$ **is possible if** $m_\phi > m_h$ **and** ξ **is not too small.**

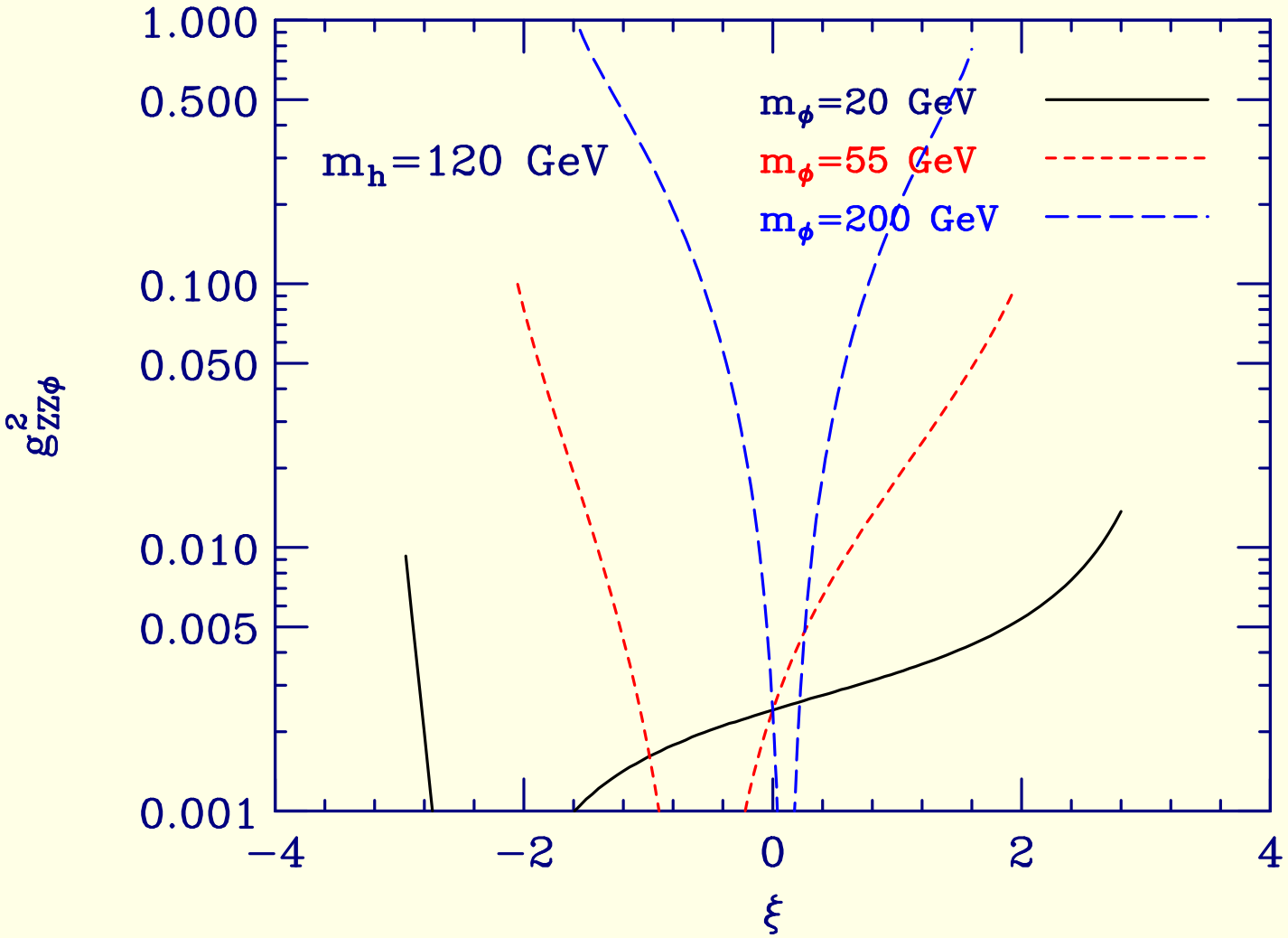

Figure 4: $g^2_{ZZ\phi}/g^2_{ZZh_{\rm SM}} = g^2_{f\bar{f}\phi}/g^2_{f\bar{f}h_{\rm SM}}$ *as a function of* ξ *for several* m_ϕ *values.*

Branching Ratios

Some important points are:

- h **branching ratios are quite SM-like (even if partial widths are different) except that** $h \to gg$ **can be bigger than normal, especially when** g^2_{fVh} **is suppressed.**

- **For** $m_\phi < 2m_W$, $\phi \to gg$ **is very possibly the dominant mode in the substantial regions near zeroes of** $g^2_{fV\phi}$.

  For $m_\phi > 2m_W$, ϕ **branching ratios are sort of SM-like (except at** $\xi \simeq 0$**) but total and partial widths are rescaled.**

LHC Capabilities

At the LHC, we (Battaglia, Dominici, de Curtis, de Roeck, JFG) focused on the case of a relatively light Higgs boson, $m_h = 120$ GeV for example.

- **The precision EW studies suggest that some of the larger $|\xi|$ range is excluded, but we studied the whole range just in case.**

- **We rescaled the statistical significances predicted for the SM Higgs boson at the LHC using the h and ϕ couplings predicted relative to the $h_{\rm SM}$.**

  A modified version of HDECAY was employed.

- **The most important modes are $gg \to h \to \gamma\gamma$ and $gg \to \phi \to ZZ^{(*)} \to 4\ell$.**

  Also useful are $t\bar{t}h$ with $h \to b\bar{b}$ and $h \to ZZ^* \to 4\ell$.

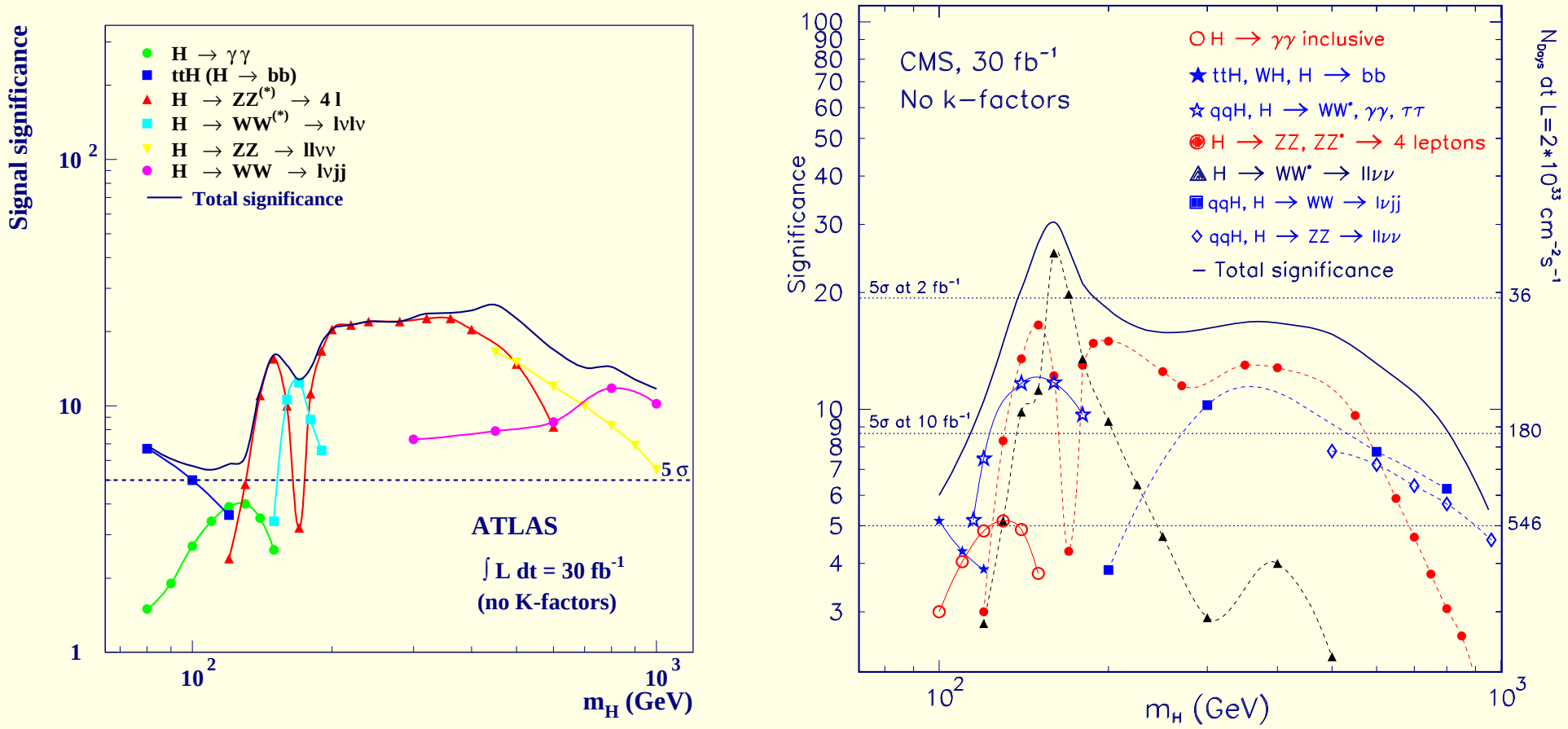

Figure 5: *SM Higgs search capabilities at the LHC for ATLAS and CMS.*

- **An example of the type of effect that will be observed is that the $h \to \gamma\gamma$ mode becomes unobservable if $|\xi|$ is large and $m_\phi > m_h$ (which together imply suppressed hWW coupling and hence suppressed W-loop**

contribution to the $\gamma\gamma h$ couplings).

One interesting graph is below. Note how we lose the $h \to \gamma\gamma$ mode if $m_\phi > m_h$, especially if $\xi < 0$. If $m_\phi < m_h$, $h \to \gamma\gamma$ will be strong if $\xi < 0$, but can be considerably weakened if $\xi > 0$.

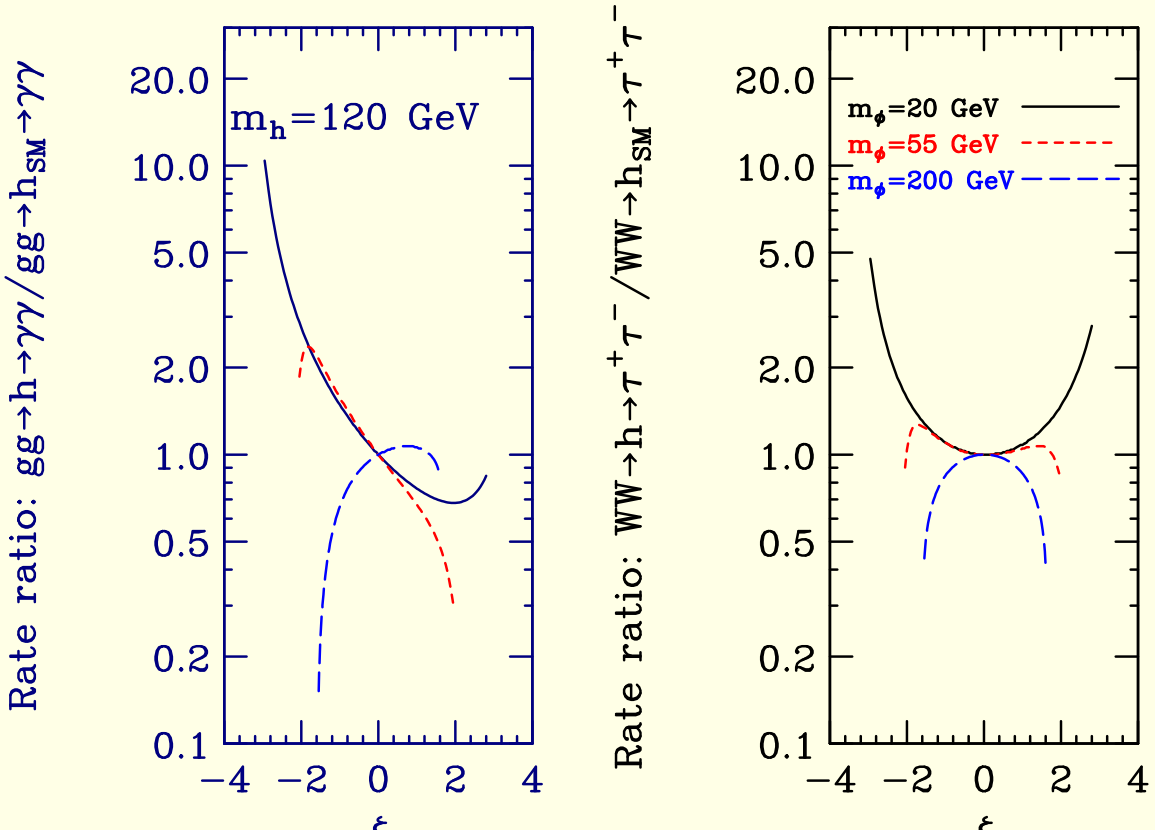

Figure 6: $gg \to h \to \gamma\gamma/gg \to h_{\rm SM} \to \gamma\gamma$ *and* $WW \to h \to \tau^+\tau^-/WW \to h_{\rm SM} \to \tau^+\tau^-$ *(same as for* $gg \to t\bar{t}h \to t\bar{t}b\bar{b}$*) for* $m_{h_{\rm SM}} = m_h$*;* $\Lambda_\phi = 5$ TeV.

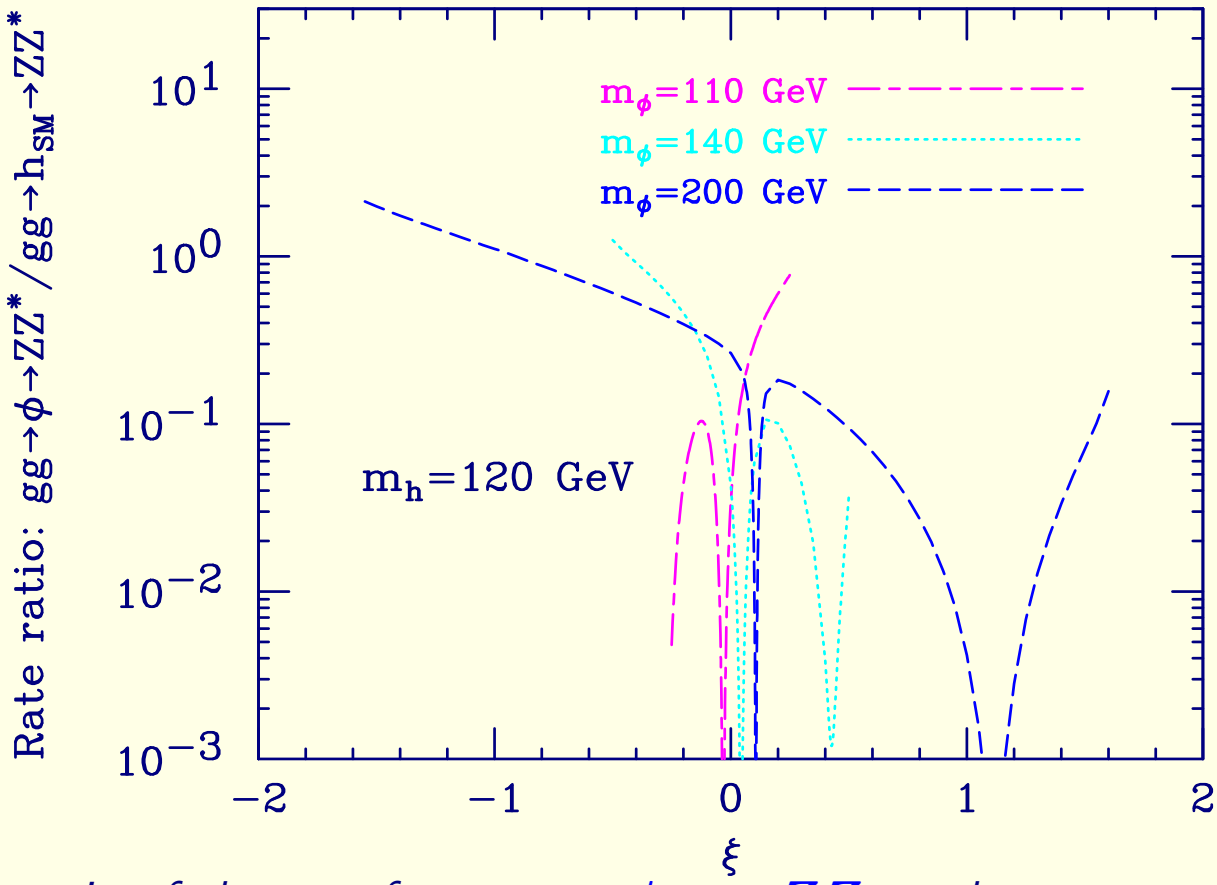

Figure 7: *The ratio of the rate for* $gg \to \phi \to ZZ$ *to the corresponding rate for a SM Higgs boson with mass* m_ϕ *assuming* $m_h = 120$ GeV *and* $\Lambda_\phi = 5$ TeV *as a function of* ξ *for* $m_\phi = 110$, 140 *and* 200 GeV. *Recall that the* ξ *range is increasingly restricted as* m_ϕ *becomes more degenerate with* m_h. *Note: for* $m_\phi > m_h$ *the mode approaches SM strength if* $\xi < 0$ *and is nearing SM strength if* $\xi > 0$ *and near maximal.*

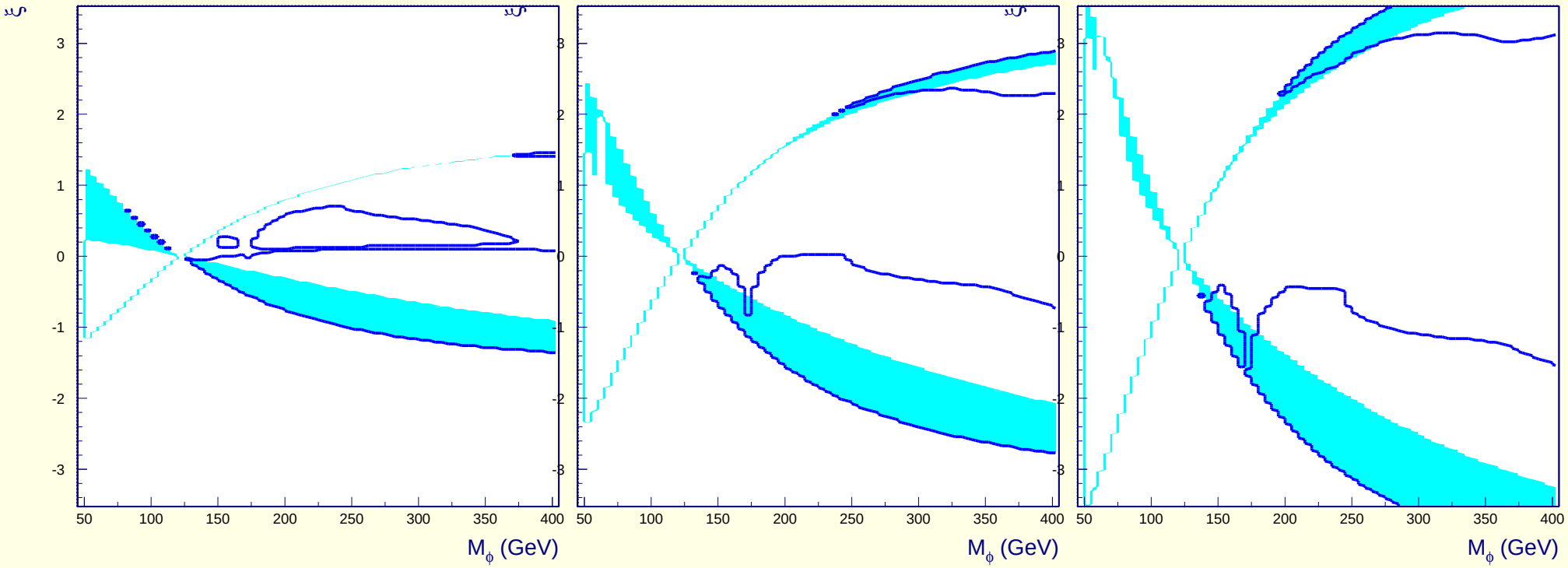

Figure 8: $L = 30\text{fb}^{-1}$ *illustration of mode complementarity at the LHC for* $m_h = 120$ GeV. *The cyan regions show where the* $gg \to h \to \gamma\gamma$ *mode (or not very important at this* m_h *value,* $gg \to h \to 4\ell$ *mode) yields a* $> 5\sigma$ *signal. The regions between dark blue curves define the regions where* $gg \to \phi \to 4\ell$ *is* $> 5\sigma$. *The graphs are for* $\Lambda_\phi = 2.5$ TeV *(left)* $\Lambda_\phi = 5$ TeV *(center) and* $\Lambda_\phi = 7.5$ TeV *(right).*

The LHC is doing pretty well except for the $m_\phi < m_h$, $\xi > 0$ and large, region.

But, some portion of this difficult region is disfavored by the precision electroweak data — e.g. $|\xi| \lesssim 1.5$ in the $\Lambda_\phi = 5$ TeV case.

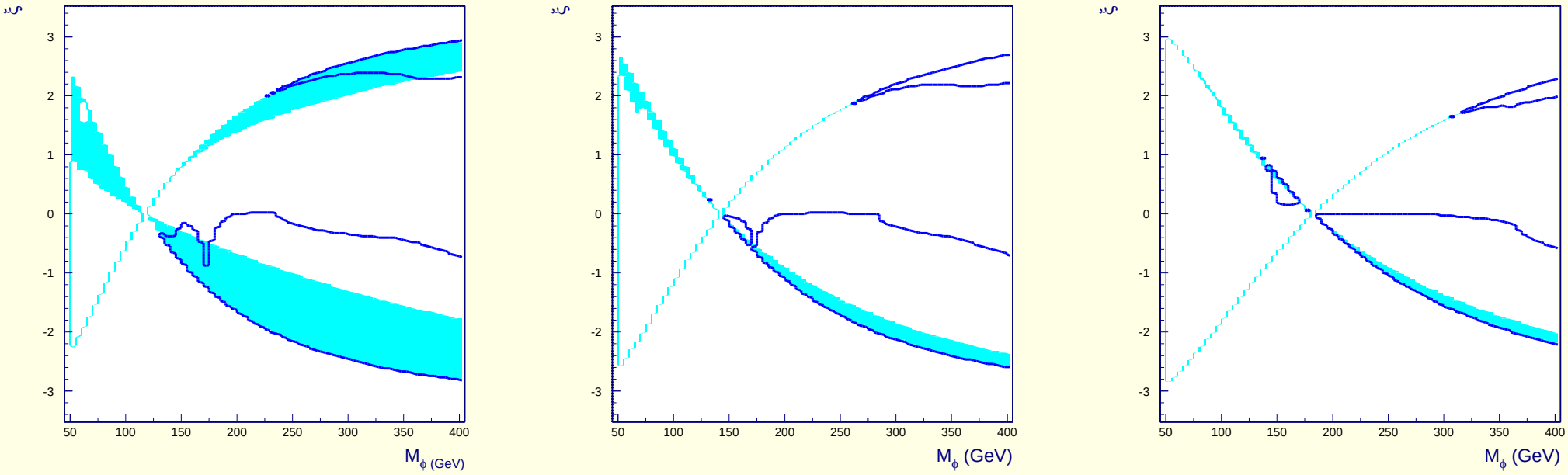

Figure 9: *As in previous figure. The graphs are for $\Lambda_\phi = 5$ TeV and $m_h = 115$ GeV (left) $m_h = 140$ GeV (center) and $m_h = 180$ GeV (right).*

Above, we see that the region where neither the h nor the ϕ can be

detected grows (decreases) as m_h decreases (increases). It diminishes as m_h increases since the $gg \to h \to 4\ell$ increases in strength at higher m_h.

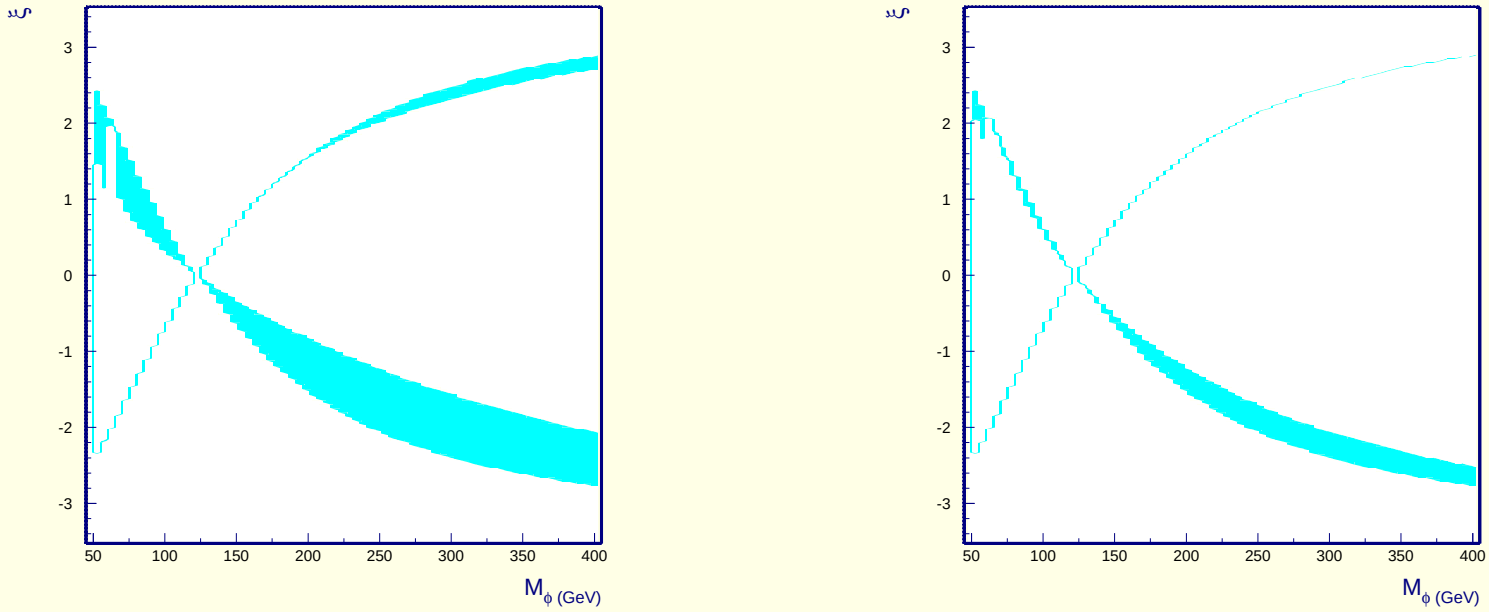

Figure 10: *The graphs are for* $\Lambda_\phi = 5$ TeV *and* $m_h = 120$ GeV *assuming LHC* $L = 30\text{fb}^{-1}$ *(left) or* $L = 100\text{fb}^{-1}$ *(right).*

The regions where the h is not observable are reduced by considering either a larger data set or qqh Higgs production, in association with forward jets. An integrated luminosity of 100 fb^{-1} would remove the regions at large positive ξ in the $\Lambda_\phi = 5$ and 7.5 TeV plots of Fig. 8. Similarly,

including the qqh, $h \to WW^* \to \ell\ell\nu\bar{\nu}$ channel in the list of the discovery modes removes the same two regions and reduces the large region of h non-observability at negative ξ values.

- Figures 8 and 9 also exhibit regions of (m_h, ξ) parameter space in which *both* the h and ϕ mass eigenstates will be detectable.

  In these regions, the LHC will observe two scalar bosons somewhat separated in mass, with the lighter (heavier) having a non-SM-like rate for the gg-induced $\gamma\gamma$ (Z^0Z^0) final state.

  Additional information will be required to ascertain whether these two Higgs bosons derive from a multi-doublet or other type of extended Higgs sector or from the present type of model with Higgs-radion mixing.

- **What about an LC?**

  An e^+e^- LC should guarantee observation of both the h and the ϕ in the region of low m_ϕ, large $\xi > 0$ within which detection of either at the LHC might be difficult. This is because the $ZZ\phi$ coupling-squared is $\gtrsim 0.01$ relative to the SM for most of this region.

  But, what if there is no LC?

$\gamma\gamma$ Collider Capabilities

- Let's remind ourselves about the SM Higgs boson with $m_h = 120$ GeV.

  After the cuts, we end up with about $S = 1450$ and $B = 335$ in the $\gamma\gamma \to h \to b\bar{b}$ channel.

  How will the CLIC module luminosity compare to that assumed in our study? We must rescale these values accordingly.

- After mixing, the S rate will be rescaled relative to B.

  The rescaling is shown in the figure.

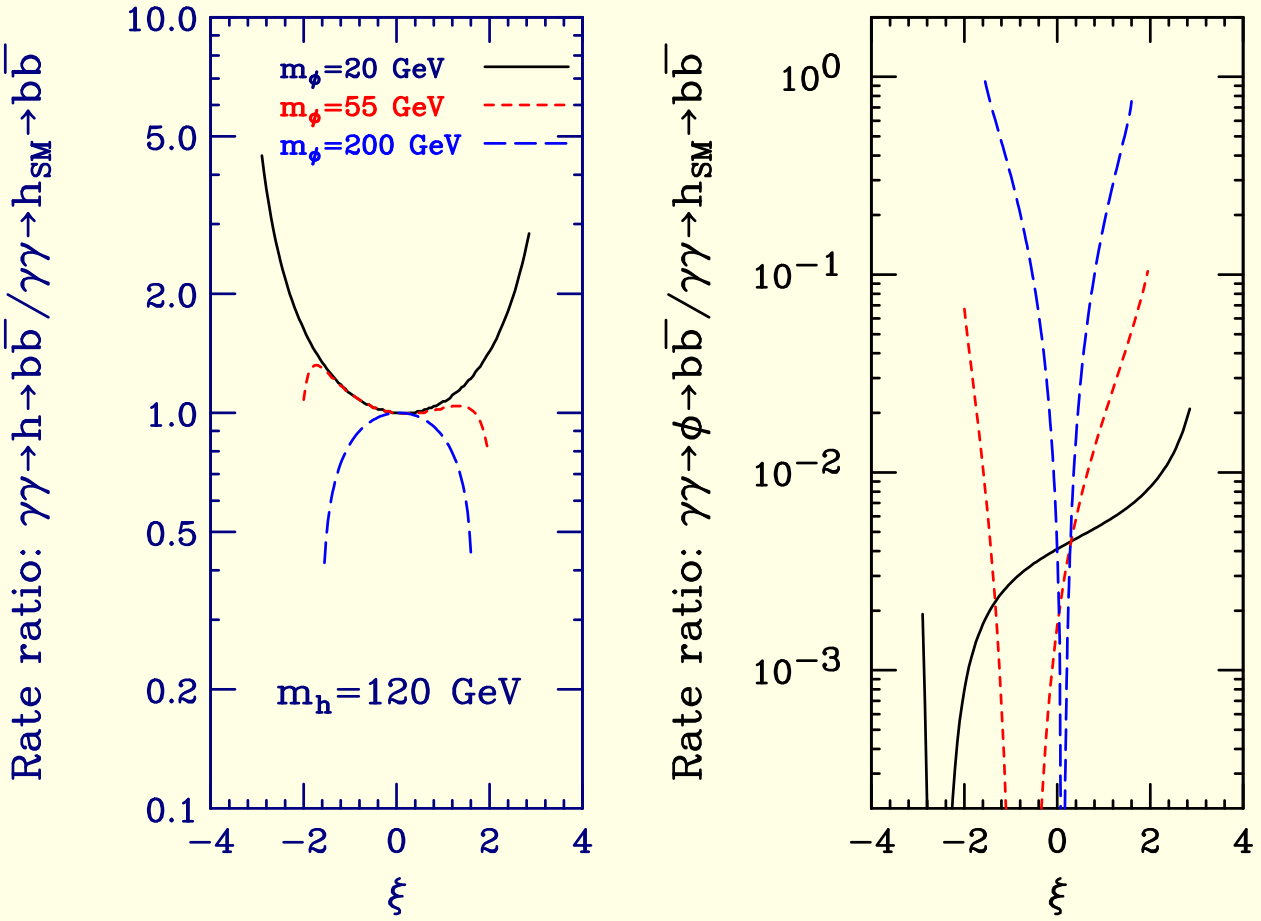

Figure 11: The rates for $\gamma\gamma \to h \to b\bar{b}$ and $\gamma\gamma \to \phi \to b\bar{b}$ relative to the corresponding rate for a SM Higgs boson of the same mass. Results are shown for $m_h = 120$ GeV and $\Lambda_\phi = 5$ TeV as functions of ξ for $m_\phi = 20$, 55 and 200 GeV.

Observe that for $m_\phi < m_h$ we have either little change or enhancement, whereas significant suppression of the $gg \to h \to \gamma\gamma$ rate was possible in this case for positive ξ.

Also note that for $m_\phi > m_h$ and large $\xi < 0$ (where the LHC could not see the h) there is much less suppression of $\gamma\gamma \to h \to b\bar{b}$ than for $gg \to h \to \gamma\gamma$ — at most a factor of 2 vs a factor of 8 (at $m_\phi = 200\ \mathrm{GeV}$).

For old L, this is no problem since $\frac{1}{2}1450/\sqrt{335} \sim 40$ is still a very strong signal.

- In fact, for old L we can afford a reduction by a factor of 16 before we hit the 5σ level!
- We can work to produce an hourglass plot for the $\gamma\gamma$ collider, but my preliminary guess is that for old L's, the $\gamma\gamma$ collider will allow h discovery (for $m_h = 120$) throughout the entire hourglass, which is something the LHC cannot do.
- Using the factor of 16 mentioned above (but this might not be the right factor — see discussion below), the ϕ with $m_\phi < 120\ \mathrm{GeV}$ will elude discovery at the $\gamma\gamma$ collider, just as at the LHC for this region.

  The only exception is the the little windows at the very largest $|\xi|$ values

for $m_\phi \geq 55$ GeV.

- Of course, we would need to have signal and background results after cuts for these lower masses to know if the factor of 16 was actually the correct factor to use.

  To get the best signal to background ratio we would want to lower the machine energy (maybe good for CLIC case?) and readjust cuts and so forth.

  This might be a useful study if there was some hope that we could improve on the factor of 16.

- For the $m_\phi > m_h$ region, we will need results for the WW and ZZ modes that are being worked on.

Conclusions

- The γC is more than competitive with the LHC for h discovery.

  The γC can see the h where the LHC can't, although the "bad" LHC regions are not very big for full L.

- Of course, there is a big part of the hourglass where the h will be seen at both colliders.

  This is most of the hourglass when L at the LHC is $> 100\text{fb}^{-1}$.

  This will certainly increase our knowledge about the h since the two rates measure different things.

  The ratio of the rates gives us $\frac{\Gamma(h\to gg)}{\Gamma(h\to b\bar{b})}$, in terms of which we may compute

$$R_{hgg} \equiv \left[\frac{\Gamma(h\to gg)}{\Gamma(h\to b\bar{b})}\right]\left[\frac{\Gamma(h\to gg)}{\Gamma(h\to b\bar{b})}\right]^{-1}_{SM}. \qquad (13)$$

  This is a very!!!! interesting number since it directly probes for the presence of the anomalous ggh coupling.

In particular, $R_{hgg} = 1$ if the only contributions to $\Gamma(h \to gg)$ come from quark loops and all quark couplings scale in the same way.

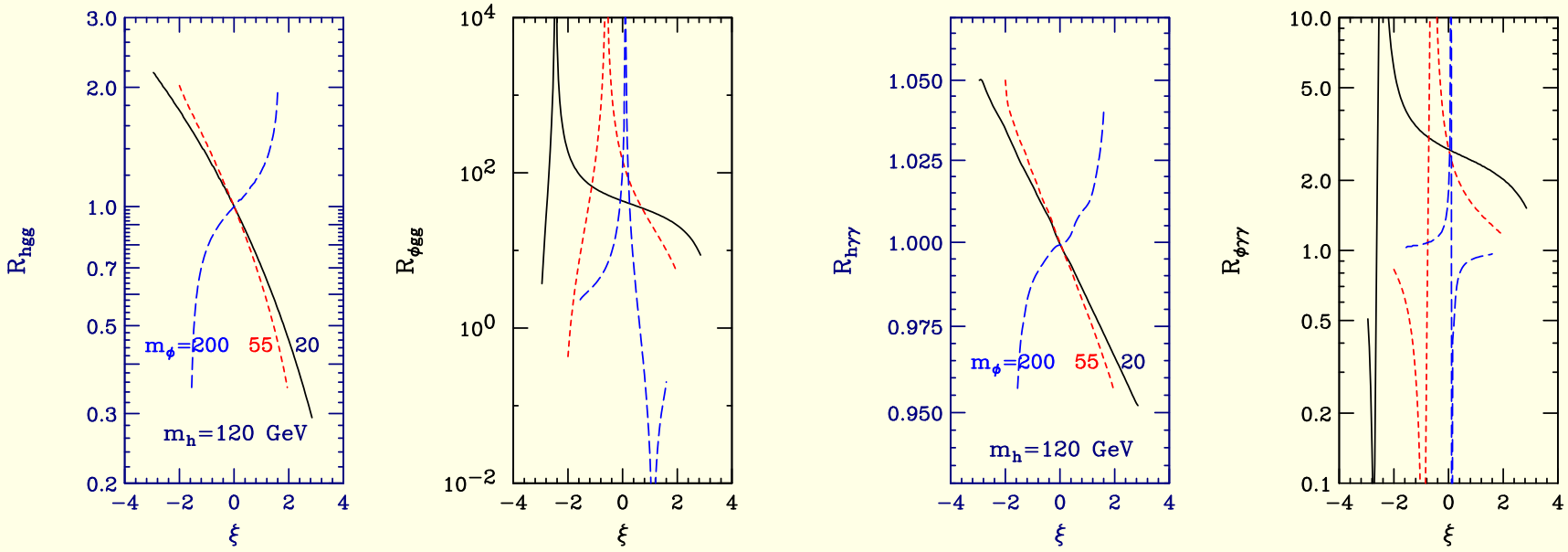

Figure 12: *In the left two plots, we give the ratios R_{hgg} and $R_{\phi gg}$ of the hgg and ϕgg couplings-squared including the anomalous contribution to the corresponding values expected in its absence. Results for the the analogous ratios $R_{h\gamma\gamma}$ and $R_{\phi\gamma\gamma}$ are presented in the two plots on the right. Results are shown for $m_h = 120$ GeV and $\Lambda_\phi = 5$ TeV as functions of ξ for $m_\phi = 20$, 55 and 200 GeV. (The same type of line is used for a given m_ϕ in the right-hand figure as is used in the left-hand figure.)*

The ability to measure R_{hgg} may be the strongest reason in the Higgs context for having the γC as well as the LHC.

Almost all non-SM Higgs theories predict $R_{hgg} \neq 1$ for one reason another, unless one is in the decoupling limit.

- Depending on L at the LHC, there is a somewhat smaller part of the hourglass (large $|\xi|$ with $m_\phi > m_h$) where *only* the ϕ will be seen at the LHC and the h will only be seen at the γC.

  (We don't know for sure about the ϕ at the γC until WW, ZZ final states are studied, but I am not all that optimistic.)

  This is a nice example of complementarity between the two machines. By having both machines we maximize the chance of seeing both the h and ϕ.

- There really does seem to be a case for the γC in the RS model context!